Fund of Catholic University Medical College, Seoul, Korea. We thank Mr. Tae-Sung Choi, NMRT for fine aerosol imaging, Mr. Hee-Duk Roh for photographic work and Miss Nam-Jee Joo for administrative assistance.

## REFERENCES

1. Fraser RG, Paré JAP. Parenchymal atelectasis. In: Fraser RG, Paré JAP, eds. *Diagnosis of diseases of the chest*. Philadelphia: W. B. Saunders; 1977:353–377.
2. Lavender JP, Irving H, Armstrong JD II. Krypton-81m ventilation scanning: acute respiratory disease. *Am J Roentgenol* 1981;136:309–316.
3. Alderson PO, Secker-Walker RH, Forrest JV. Detection of obstructive pulmonary disease. *Radiololgy* 1974;111:643–648.
4. Kotrappa P, Raghunath B, Subramanyam PPS, et al. Scintigraphy of lungs with dry aerosol-generation and delivery system. *J Nucl Med* 1977;18:1082–1085.
5. Soni PS, Raghunath B. Generation of aerosols: BARC nebulizer and others. In: Bahk YW, Isawa T, eds. *Radioaerosol imaging of the lung*. Vienna: International Atomic Energy Agency Publication; 1994:24–42.
6. Bahk YW, Chung SK. Radioaerosol lung scanning in chronic obstructive pulmonary disease (COPD) and related disorders. In: Bahk YW, Isawa T, eds. *Radioaerosol imaging of the lung*. Vienna: International Atomic Energy Agency Publication; 1994:88–135.
7. Isawa T, Teshima T, Hirano T, et al. Mucociliary clearance and transport in bronchiectasis: global and regional assessment. *J Nucl Med* 1990;31:543–548.
8. Hayes M, Taplin GV. Lung imaging with radioaerosols for the assessment of airway disease. *Semin Nucl Med* 1980;10:243–251.
9. Boxen I, Zhang ZM. Deposition of radioaerosol throughout the major airways in tracheobronchitis. *Clin Nucl Med* 1990;15:703–704.

# Background Subtraction in Technetium-99m-MAG3 Renography

Andrew Taylor, Jr, Killol Thakore, Russell Folks, Raghuveer Halkar and Amita Manatunga
*Division of Nuclear Medicine, Department of Radiology, Emory University School of Medicine, Atlanta, Georgia; and Louisiana State University Medical Center, New Orleans, Louisiana*

Correction represents a potential source of error in estimating split renal function and camera-based clearances. The purpose of this study was to determine which of five background options and four time intervals was associated with the least error for $^{99m}$Tc-mercaptoacetyltriglycine (MAG3). **Methods:** Fifteen single-kidney patients were imaged supine after 111–370 MBq (3–10 mCi) $^{99m}$Tc-MAG3 injection. A phantom kidney was drawn on the 2–3-min images, approximately equal in size to the solitary kidney and used for all time intervals. Counts in the phantom and native kidneys were calculated using manual inferior and lateral regions of interest (ROIs), automated elliptical and perirenal background ROIs and no background correction at various time intervals (1–2, 1–2.5, 1.5–2.5 and 2–3 min) postinjection. With optimal background correction, counts and the relative function in the phantom kidney should be zero. The error was measuring by estimating both the relative function and absolute function expressed as the percent injected dose in the phantom kidney. **Results:** The percent injected dose in the phantom kidney as well as the error in measuring relative function were significantly greater than zero for the inferior background correction and the no background correction options at all time intervals, $p < 0.05$. The percent dose in the kidney and the error associated with the lateral, elliptical and perirenal ROIs were not significantly different from zero. **Conclusion:** Regardless of time interval, the greatest error was associated with no background correction. The inferior ROI consistently underestimated the background correction and probably should not be used for $^{99m}$Tc-MAG3. There was no significant difference between errors generated using the lateral and automated ROIs, although automated ROIs are probably more reproducible for sequential studies.

**Key Words:** background correction; relative renal function; regions of interest

**J Nucl Med 1997; 38:74–79**

Radionuclide renograms should routinely include a measurement of relative renal function (*1–3*). Most commercial software programs make this measurement during the 1–2- or 2–3-min interval after radiopharmaceutical injection. Moreover, camera-based methods are available to calculate the glomerular filtration rate (GFR), effective renal plasma flow (ERPF) and $^{99m}$Tc-mercaptoacetyltriglycine (MAG3) clearance based on the percent of the injected dose of $^{99m}$Tc-diethylenetriaminepentaacetic acid (DTPA), [$^{131}$I]ortho-iodohippurate (OIH) or MAG3 in the kidneys at 1–2, 1–2.5 or 2–3 min postinjection (*4–6*). Measurements of relative renal function and gamma camera based clearance measurements are usually corrected for background and results may differ depending on the background region selected. Controversy exists not only with the method and region of interest (ROI) used for background correction but also whether or not background subtraction is even needed (*2,7–11*). Some authors suggest that, at relative good levels of renal function, the use of background subtraction introduces more problems than it solves and that it is virtually impossible, short of removing the kidney, to determine the true background contribution in any given individual at a given time (*2,9*). Finally, results obtained with $^{99m}$Tc-DTPA or OIH may not be applicable to MAG3 due to its higher protein binding and lower volume of distribution.

To better evaluate the most appropriate background ROI for patients undergoing $^{99m}$Tc-MAG3 renography, a study was done to estimate relative renal function in a series of 15 patients with unilateral nephrectomies. A phantom kidney was drawn approximately equal in size to the solitary kidney. The goal of the study was to evaluate the effects of various background options (no background, elliptical, perirenal, inferior and lateral backgrounds) on both the relative function and the $^{99m}$Tc-MAG3 clearance in the phantom kidney at various time intervals postinjection (1–2,1–2.5,1.5–2.5 and 2–3 min, respectively).

## MATERIALS AND METHODS

Following intravenous administration of 3–10 mCi (111–370 MBq) $^{99m}$Tc-MAG3, images were acquired posteriorly at 2 sec/frame for 24 frames, 15 sec/frame for 16 frames and 30 sec/frame for 40 frames with patients in the supine position. Data were acquired using a gamma camera equipped with 400 mm crystal and a low-energy, all-purpose, parallel-hole (LEAP) collimator and processed using the QuantEM™ software (Emory

Received June 20, 1995; revision accepted June 22, 1996.
For correspondence or reprints contact: Andrew Taylor, Jr, MD, Division of Nuclear Medicine, Department of Radiology, Emory University School of Medicine, 1364 Clifton Rd., NE, Atlanta, GA 30322.

**TABLE 1**
Age, Sex, Technetium-99m-MAG3 Clearance and Location of the Phantom Kidney

| Patient no. | Age | Sex | MAG3 clearance (ml/min) | Phantom kidney |
|---|---|---|---|---|
| 1 | 48 | F | 49 | L |
| 2 | 36 | M | na | L |
| 3 | 76 | F | 48 | R |
| 4 | 76 | M | 59 | R |
| 5 | 64 | F | 90 | R |
| 6 | 62 | F | 210 | R |
| 7 | 34 | F | 84 | L |
| 8 | 69 | M | 135 | R |
| 9 | 55 | M | 167 | R |
| 10 | 37 | F | 192 | R |
| 11 | 32 | F | 90 | R |
| 12 | 32 | M | 58 | R |
| 13 | 63 | F | 92 | L |
| 14 | 75 | F | 115 | R |
| 15 | 37 | M | 307 | R |

na = not available. The $^{99m}$Tc-MAG3 clearance in this table is based on the single-sample technique (*12,13*).

University, Atlanta, GA). The photo peak was selected at 140 keV with a 20% window. The single sample technique (*12,13*) was used to calculate the total $^{99m}$Tc-MAG3 clearance listed in Table 1.

Fifteen patients (9 women, 6 men; age range 32–76 yr; mean age 53 yr) with a solitary kidney comprised the study group. Eleven patients had right nephrectomy, while four had a left nephrectomy. ROIs were drawn around the solitary kidney, and a phantom kidney ROI was drawn on the contralateral side approximately equal in size to the solitary kidney ROI. Relative function was calculated, without background correction and with background correction, using automated elliptical, automated perirenal and manual inferior and lateral ROIs on the 2–3-min images (Fig. 1).

The elliptical background ROI was generated by first drawing an imaginary box around the limits of the kidney using the kidney ROI. The pixel coordinates were used to define the width and height of the box. Since an ellipse requires a major and minor axis, the major axis of the inner ellipse was the length of the box plus four pixels, and the minor axis was the width of the box plus four pixels. For the outer ellipse, the major axis was the major axis of the inner ellipse plus three pixels; the minor axis was the minor axis of the inner ellipse plus three pixels. The inner ellipse was subtracted from the outer ellipse to determine the background ROI.

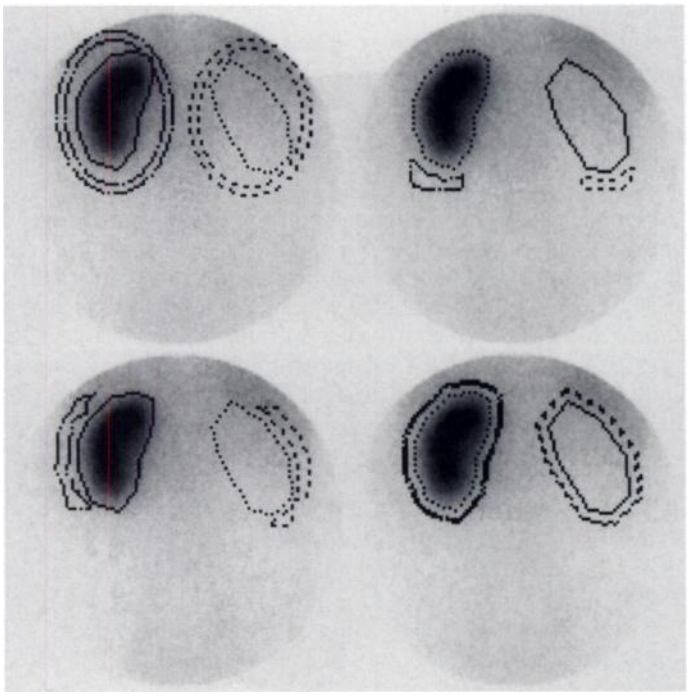

**FIGURE 1.** Background ROI. Elliptical (upper left), inferior (upper right), lateral (lower left), perirenal (lower right).

The perirenal ROI was two pixels wide and one pixel outside the kidney ROI. The program was developed by Tom Ahrén of Vasteras, Sweden, for a 64 × 64 format and was placed in the General Electric European Library of User Developed Software. The version we used was modified for a 128 × 128 matrix by Stefan Ekberg, Linköping, Sweden, which is similar to the program evaluated for $^{99m}$Tc-DTPA by Moonen and Granerus (*14*).

A pilot study was performed using only the 2–3-min interval with each of the 15 studies processed by two observers (KT and RF). Subsequently, each of the 15 studies was independently processed by two observers (RF and RH) for all four time intervals using the same kidney ROIs. For each background region, the average counts/pixel were multiplied by the number of pixels in the renal ROI and then subtracted from the counts in the renal ROI. In the preliminary study, the error (%) associated with the 2–3-min interval was calculated by dividing the background corrected counts in the phantom kidney by the background corrected counts in the patient's kidney and multiplying by 100. This method of error calculation corresponds to the approach used in clinical practice; however, the denominator varied with each different background ROI and because the denominator varied, it was difficult to compare results using different background ROIs. To avoid this problem and obtain a better comparison of the magnitude of the error in measuring relative function, the background corrected counts in the phantom kidney for each ROI were divided by the average of the four background corrected counts in the patient's native kidney and then multiplied by 100.

The error calculations described above provide a measure of the error which might occur in measuring relative function. If, however, a patient's renal function approached zero, error in measuring relative renal function could be quite large, but it would have little clinical relevance. To address this issue, we calculated the magnitude of the error in terms of the percent of the injected dose in the phantom kidney for 14 of the 15 patients whose injected dose was counted on the computer. Using the percent dose in the phantom kidney at 1–2, 1–2.5 and 2–3 min and previously published regression equations (*6*), the percent dose in the phantom kidney was converted to a $^{99m}$Tc-MAG3 clearance in milliliter per minute to provide a functional index of the magnitude of the error.

### Statistical Methods

An average error was calculated for each ROI for each subject by averaging the values obtained by the two observers. Two outcome variables were considered: error and the absolute error of the counts in the phantom kidney (see Results). A repeated measure analysis of variance was used to determine whether there was a difference between the background ROI options at each time period. For each ROI option and time period, confidence intervals were calculated. Boneferroni adjustments were made to confidence intervals to assure the overall 95% probability coverage (*15*). Confidence limits were based on all comparison data in a particular dataset; consequently, the 95% confidence intervals for the inferior and no background ROI options differ in Tables 2, 3, 4 and 5 even though the means are the same. An interval containing zero would indicate that the true mean value of the error was not significantly

**TABLE 2**
Estimates of the Percent Function Associated with the Phantom Kidney Expressed as the Mean Error with 95% Confidence Intervals in Parentheses*

| | 1–2 min | 1–2.5 min | 1.5–2.5 min | 2–3 min |
|---|---|---|---|---|
| No background | 45†(30,59) | 41†(28,55) | 38†(26,51) | 35†(23,47) |
| Elliptical | −9 (−23,6) | −8 (−21,6) | −7 (−19,6) | −6 (−18,6) |
| Inferior | 17† (3,31) | 15†(2,29) | 14†(1,26) | 12†(0,24) |
| Lateral | −6 (−21,8) | −6 (−19,8) | −5 (−17,8) | −5 (−17,7) |
| Perirenal | −6 (−21,8) | −6 (−19,8) | −5 (−18,7) | −6 (−18,7) |

*The mean error (%) provides an estimate of the relative uptake in the phantom kidney and was calculated by dividing the background corrected counts in the phantom kidney by the average of the four background corrected counts in the native kidney and multiplying by 100. A priori, the relative uptake in the phantom kidney should be zero because background corrected counts in the phantom kidney should be zero.

†Significantly greater than zero, $p < 0.05$.

different from zero ($p < 0.05$). When comparing two ROIs, the Tukey's LSD procedure was used (*15*).

## RESULTS

Interobserver variability was tested in a pilot study by having the two different observers (KT and RF) process the 2–3-min data. Subsequently, two different observers (RH and RF) processed the studies for all four time intervals using the same renal and phantom kidney ROIs. There was little interobserver variability for the inferior and lateral ROIs (intraclass correlation = 0.95). Not surprisingly, there was no interobserver variability associated with the automated ROIs. The results of the two observers were then averaged for the final data analysis. The phantom kidney was the left kidney in four patients and the right kidney in 11 patients. We evaluated our data to test if there was a difference in the results obtained from the right and left phantom kidneys using the different background options at the different time periods. There was no difference in the results from the right and left phantom kidneys; consequently, data from all 15 patients were pooled for the subsequent data analysis.

Patient characteristics are listed in Table 1. Background correction can be either overestimated or underestimated; both are errors. For this reason, we chose to present our data using both the mean error and mean error of the absolute value (absolute mean error). The difference can be illustrated by considering the following example: an overestimation of background by 40% and an underestimation of background by 40% in two successive patients would represent a mean error of 0% and an absolute mean error of 40% (the absolute mean error illustrates the bias in the technique).

**TABLE 3**
Estimates of the Percent Function Associated with the Phantom Kidney Expressed as the Absolute Value of Mean Error with 95% Confidence Intervals*

| | 1–2 min | 1–2.5 min | 1.5–2.5 min | 2–3 min |
|---|---|---|---|---|
| No background | 45† (37,52) | 41† (34,48) | 38† (31,45) | 35† (28,41) |
| Elliptical | 11 (3,19) | 10 (3,17) | 9 (2,16) | 8 (1,14) |
| Inferior | 17 (9,25) | 15 (8,23) | 14 (7,20) | 12 (5,18) |
| Lateral | 10 (3,18) | 9 (2,17) | 8 (2,15) | 8 (1,15) |
| Perirenal | 8 (0,16) | 7 (0,14) | 6 (−1,13) | 7 (0,13) |

*The absolute error (%) provides an estimate of the bias in the measurement of the relative uptake in the phantom kidney and was calculated by dividing the absolute value of background corrected counts in the phantom kidney by the average of the four background corrected counts in the native kidney and multiplying by 100.

†The absolute value associated with no background correction is higher than the absolute value associated with any of the four background corrections ($p < 0.05$).

In the pilot study, error was calculated using the 2–3-min interval by dividing the background corrected counts in the phantom kidney by the background corrected counts in the patient's kidney. With no background correction, the absolute mean error averaged 31.7% compared with 16.3%, 8.7%, 8.0% and 5.3% for inferior, lateral, elliptical and perirenal ROI background correction, respectively. Furthermore, the mean errors associated with no background correction or an inferior background correction (31.7% ± 16.7% and 16.3% ± 10.9%, respectively) were both significantly greater than zero, $p < 0.0001$, and both consistently underestimated the background correction compared to the lateral and automated ROIs ($p < 0.005$). The mean error and s.d. of the perirenal, lateral and elliptical ROIs were −1.3% ± 6.7%, −1.2% ± 8.1% and −2.1% ± 9.9%, respectively; none of them were significantly different from zero nor were they significantly different from each other. The lowest error was associated with the perirenal ROI, although there was no significant difference in the results using the lateral and two automated ROIs.

Failure to correct for background clearly led to the poorest results, and this difference was highly significant. However, this method of background subtraction led to a varying denominator and limited our ability to compare the magnitude of the error associated with the different background techniques. Since our goal was to determine the best background ROI, and since, therefore, we could not claim to know the answer a priori, we averaged the background corrected counts in the native kidney using the inferior, lateral, perirenal and elliptical regions of interest and used this average as a constant denominator to determine percent relative uptake in the phantom kidney. The no background value was not averaged with the others because the data in our pilot study had clearly shown the necessity of background subtraction.

The mean error (%) in the relative function calculation associated with the phantom kidney is presented in Table 2 and is illustrated for the 1–2.5-min interval in Figure 2. The results obtained using a standardized denominator for all four time intervals were essentially the same as those obtained in the pilot study with the errors associated with the inferior background ROI or no background correction both significantly greater than zero ($p < 0.05$). There was no significant difference between the errors associated with the elliptical, perirenal or inferolateral backgrounds, and these results were not significantly different from zero. The absolute mean error (Table 3) demonstrates the bias associated with each background option. The bias associated with no background was significantly greater than that of the four background options, $p < 0.05$; however, there was no significant difference in the bias associated with the four background ROIs.

Table 4 presents the mean percent dose in the phantom kidney at 1–2, 1–2.5, 2–3-min postinjection and the corresponding $^{99m}$Tc-MAG3 clearances. Figure 3 illustrates the data for the 1–2.5-min interval. Once again, the percent dose in the kidney using no background correction or an inferior background correction was significantly greater than zero at all three intervals, $p < 0.05$. The percent dose in the kidney at 1–2, 1–2.5 and 2–3 min was converted into a corresponding $^{99m}$Tc-MAG3 clearance using a published regression equation to provide an

**TABLE 4**
Mean Percent Injected Dose in the Phantom Kidney with 95% Confidence Limits in Parentheses and Corresponding Technetium-99m-MAG3 Clearance (ml/min)*

| | 1–2 min | | 1–2.5 min | | 2–3 min | |
|---|---|---|---|---|---|---|
| | % dose | MAG3 CL | % dose | MAG3 CL | % dose | MAG3 CL |
| No background | 2.6* (2.1,3.2) | 48.6 | 3.3* (2.6,4.0) | 32.7 | 2.6* (2.0,3.1) | 29.0 |
| Elliptical | −0.5 (−1.1,0) | −7.1 | −0.6 (−1.3,0.1) | −9.4 | −0.4 (−1.0,0.1) | −10.4 |
| Inferior | 1.0* (0.5,1.6) | 20.6 | 1.3* (0.6,1.9) | 11.0 | 0.9* (0.4,1.4) | 7.3 |
| Lateral | −0.3 (−0.9,0.3) | −3.8 | −0.3 (−1.0,0.4) | −7.1 | −0.2 (−0.8,0.3) | −9.4 |
| Perirenal | −0.4 (−0.9,0.2) | −2.6 | −0.4 (−1.1,0.3) | −6.1 | −0.4 (−0.9,0.2) | −7.8 |

*For purposes of this table, the percent dose has been rounded off to the nearest 0.1%; the $^{99m}$Tc-MAG3 clearance was calculated using the original data. The mean percent dose in the phantom kidney using no background correction or an inferior background correction was significantly greater than zero ($p < 0.05$).

index of the magnitude of the error (*6*). The percent dose at 1.5–2.5 min was not included because there is no published regression equation converting this value to a $^{99m}$Tc-MAG3 clearance. The regression equations were not constrained to go through zero and contained constants of 2.5, −2.5 and −4.7 for the 1–2, 1–2.5 and 2–3-min regression equations, respectively; these constants somewhat distort the results for clearances close to zero. Failure to correct for background led to an error of 48.6 ml/min for the 1–2-min interval and 32.7 and 29 ml/min for the 1–2.5- and 2–3-min intervals, respectively. Based on a normal $^{99m}$Tc-MAG3 clearance in subjects under age 40 of 304 ml/min (*16*), these values represent errors in the range of 10%–15%.

## DISCUSSION

We selected a patient population with unilateral nephrectomies because we knew a priori that the relative function was 0% and 100% in this patient population, and this a priori knowledge allowed us to estimate the error associated with different background corrections. More complex methods of background correction have been developed which incorporate data from a precordial curve. However, Tondeur et al. (*17*) reported that the precordial $^{99m}$Tc-MAG3 curve does not match the plasma disappearance curve, and we have confirmed those observations (unpublished data). Consequently, more complex methods of background correction which employ a precordial curve to correct for intravascular $^{99m}$Tc-MAG3 activity are unlikely to represent a major improvement over the simpler background correction described in this article.

As expected, there was no interobserver variation when the automated ROIs were selected; however, there was a high correlation between the two observers when the inferior and lateral background ROIs were drawn manually. In our study, all observers had worked closely together and had been given a template showing how to draw the inferior and lateral ROIs. There would likely be much more variation between individuals at different institutions or even between different individuals at the same institution unless there were a clearly defined protocol for drawing manual ROIs.

It could be argued that the backgrounds described in this article overcorrect because they fail to take into account the attenuation of background activity which would have occurred if a kidney had been present. Counter to this argument is the fact that the error associated with the elliptical, perirenal and lateral ROIs were not significantly different from zero. It is also important to note that the kidney itself is a source of background activity, and this intrarenal background activity probably compensates for any overcorrection by perirenal or elliptical backgrounds. Intrarenal background activity is activity in the kidney which does not reflect the renal functional parameter being measured; the primary intrarenal background sources are vascular and interstitial activity. Vascular and interstitial activity vary with time, radiopharmaceutical and from one individual to another (*10*).

Background correction assumes an increasing importance as renal function deteriorates and is a necessary component of camera-based techniques to calculate relative renal function and to estimate renal clearances. Extrarenal background is dependent on the position of the kidneys in relation to the liver and other abdominal organs, whose size and location may vary from patient to patient (*18*). Since the location of the kidneys varies slightly from patient to patient with variable superimposition of the kidney over the liver and spleen, a perirenal or elliptical background ROI will change the background correction accord-

**TABLE 5**
Percent Injected Dose (Absolute Value) in the Phantom Kidney with 95% Confidence Limits in Parentheses and Corresponding Technetium-99m-MAG3 Clearance (ml/min)*

| | 1–2 min | | 1–2.5 min | | 2–3 min | |
|---|---|---|---|---|---|---|
| | % dose | MAG3 CL | % dose | MAG3 CL | % dose | MAG3 CL |
| No background | 2.6* (2.1,3.2) | 48.6 | 3.3* (2.6,3.9) | 32.7 | 2.6* (2.1,3.1) | 29.0 |
| Elliptical | 0.6 (0,1.1) | 12.3 | 0.7 (0,1.3) | 4.6 | 0.5 (−0.1,1.0) | 1.2 |
| Inferior | 1.0 (0.5,1.6) | 20.6 | 1.3 (0.6,1.9) | 11.0 | 0.9 (0.4,1.4) | 7.3 |
| Lateral | 0.4 (−0.1,1.0) | 10.1 | 0.5 (−0.1,1.2) | 3.1 | 0.4 (−0.1,0.9) | 0.4 |
| Perirenal | 0.4 (−0.2,0.9) | 8.8 | 0.4 (−0.2,1.1) | 2.2 | 0.4 (−0.2,0.9) | 0.0 |

*For purposes of this table, the absolute value of percent dose has been rounded off to the nearest 0.1%; the $^{99m}$Tc-MAG3 clearance was calculated using the original data. The 95% confidence limits are in parentheses. The absolute value with no background correction is significantly higher than the absolute value associated with any of the four background corrections ($p < 0.05$).

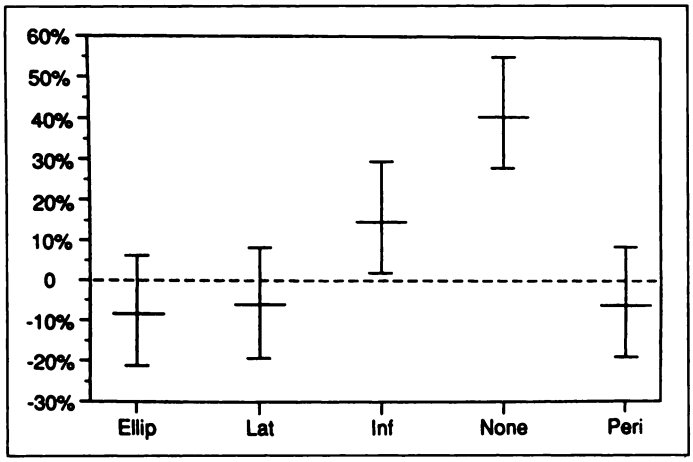


**FIGURE 2.** Mean error and 95% confidence limits for elliptical (Ellip), lateral (Lat), inferior (Inf), no (None) and perirenal (Peri) background regions of interest at 1–2.5 min postinjection. The values obtained without background correction or using an inferior background correction were both significantly greater than zero ($p < 0.05$).

ingly. Selection of a background ROI slightly separated from the kidney minimizes the inclusion of renal activity in the background ROI. Gates (*4*) compared inferolateral and ring background corrections and reported slightly better results for the inferolateral background, although the differences were not significant. Several investigators have chosen to use ring or perirenal background ROIs for $^{99m}$Tc-DTPA renography (*19,20*). Peters et al. (*21,22*) evaluated background correction in more detail and reported that a perirenal ROI was superior to subrenal or suprarenal ROI for background correction of $^{99m}$Tc-DTPA studies. Moonen and Granerus confirmed these results for $^{99m}$Tc-DTPA and recommended a perirenal background area two pixels wide and one pixel away from the kidney (*14*). Radiopharmaceuticals with minimum protein binding such as $^{99m}$Tc-DTPA have a much greater interstitial component than more highly protein-bound tracers such as $^{99m}$Tc-MAG3 (*23*). Consequently, the effects of protein binding could affect the choice of background; however, our results suggest that an elliptical or perirenal background ROI is also an appropriate choice for MAG3.

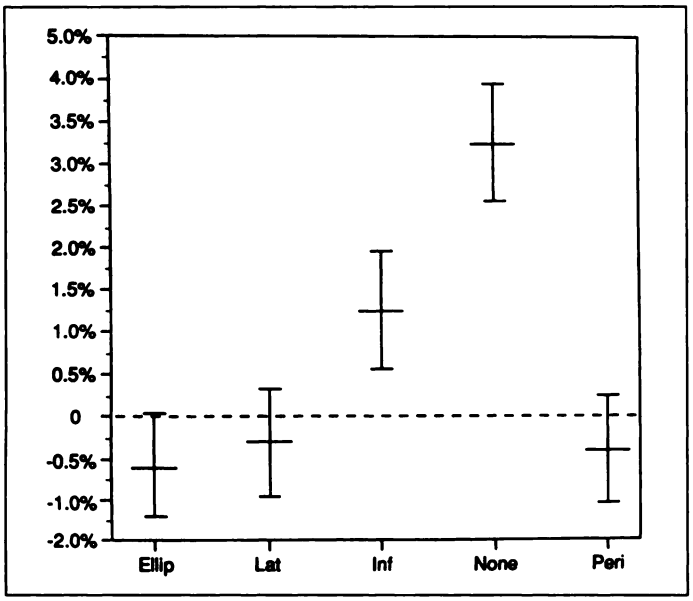


**FIGURE 3.** Mean percent injected dose in the phantom kidney and 95% confidence limits for elliptical (Ellip), lateral (Lat), inferior (Inf), no (None) and perirenal (Peri) background ROI at 1–2.5 min postinjection. The values obtained without background correction or using an inferior background correction were both significantly greater than zero ($p < 0.05$).

An automated background ROI generated on the 1–2- or 2–3-min images may overestimate background at later time periods if there is overlap of the background ROI with a dilated renal pelvis, ureter or, in the case of transplants, bladder. This overlap would not affect measurements of relative function or camera-based clearance measurements during the 1–3-min time period but could distort the latter portion of the renogram curve. Automated background correction software should automatically exclude the areas of the renal pelvis or ureter or allow the operator to modify the background ROI if the background ROI overlaps substantial activity in a dilated pelvis or ureter.

Finally, the study was also designed to help determine which time intervals would be most appropriate for measurement of a $^{99m}$Tc-MAG3 clearance using a camera-based technique. Based on a consideration of backgrounds alone, there was no significant difference in the results. Furthermore, a previous study comparing a multisample $^{99m}$Tc-MAG3 clearance with percent dose in the kidney at 1–2, 1–2.5 and 2–3 min postinjection showed no significant diffference in the regression equations for the three time intervals (*6*). However, in a well-hydrated patient, $^{99m}$Tc-MAG3 may enter the urine and washout of the kidney ROI within 3 min of injection; consequently, most experienced observers recommend making the measurement at 1–2 or 1–2.5 min postinjection (*24*). Some investigators have recommended using a relatively low dose (1.0 mCi) of $^{99m}$Tc-MAG3 (*24,25*). If a low dose is used, counting statistics will be improved by extending the intervals. Consequently, we chose to illustrate the 1–2.5-min data in Figures 3 and 4.

## CONCLUSION

Our results support the need for background correction. The inferior ROI underestimated background correction compared to the other ROIs and is probably not acceptable for $^{99m}$Tc-MAG3. There was no significant difference between the lateral and automated ROIs; however, the automated perirenal and elliptical ROIs are more reproducible than the lateral ROI and these automated ROIs will probably minimize interobserver and intraobserver variability.

## ACKNOWLEDGMENT

We would like to express our appreciation to Charlotte Berry for assistance with the manuscript.

## REFERENCES

1. Taylor A Jr, Nallly JV. Clinical applications of renal scintigraphy. *Am J Roentgenol* 1995;164:31–41.
2. Blaufox MD. Procedures of choice in renal nuclear medicine. *J Nucl Med* 1991;32: 1301–1309.
3. Russell CD, Young D, Billingsley JD, Dubovsky EV. Technical procedures for use of the new kidney agent technetium-99m-MAG3. *J Nucl Med Technol* 1992;19:147–152.
4. Gates GF. Glomerular filtration rate: estimation from fractional renal accumulation of $^{99m}$Tc-DTPA (stannous). *Am J Roentgenol* 1982;138:565–570.
5. Schlegel JU, Halkiopoulos HL, Prima R. Determination of filtration fraction using the gamma scintillation camera. *J Urol* 1979;14:417–420.
6. Taylor A, Corrigan P, Galt J, et al. Measurement of the clearance of $^{99m}$Tc-MAG3 using an improved camera based method to calculate $^{99m}$Tc-MAG3 clearance. *J Nucl Med* 1995;36:1689–1695.
7. Fine EJ, Axelrod M, Gorkin J, et al. Measurement of effective renal plasma flow: comparison of methods. *J Nucl Med* 1987;28:1393–1400.
8. Decostre P, Salmon Y Ham HR, Piepsz A. Procedures of choice in nuclear medicine [Letter]. *J Nucl Med* 1992;33:175.
9. Blaufox MD. Procedures of choice in nuclear medicine [Letter]. *J Nucl Med* 1992;33:175–176.
10. Piepsz A, Dobbeleir A, Ham HR. Effect of background correction on separate technetium-99m-DTPA renal clearance. *J Nucl Med* 1990;31:430–435.
11. Inoue Y, Machida K, Honda N, Takahashi T, Mamiya T. Background correction in estimating inital renal uptake-comparison between $^{99m}$Tc-MAG3 and $^{99m}$Tc- DTPA. *Clin Nucl Med* 1994;19:1049–1054.
12. Taylor A Jr, Corrigan P, Eshima D, Folks R. Prospective validation of a single sample technique to determine $^{99m}$Tc-MAG3 clearance. *J Nucl Med* 1992;33:1620–1622.

13. Russell CD, Taylor A, Eshima D. Estimation of technetium-99m-MAG3 plasma clearance in adults from one of two blood samples. *J Nucl Med* 1989;30:1955–1959.
14. Moonen M, Granerus G. Subtraction of extra-renal background in $^{99m}$Tc-DTPA renography: comparison of various regions of interest. *Clin Phys* 1992;12:453–461.
15. Neter J, Wasserman W, Kutner M. *Applied linear statistical models*, 3rd ed. Homewood, IL: Irwin Publishing Company; 1990.
16. Russell CD, Li L, Kahraman HN, Dubovsky EV. Renal clearances of technetium-99m-MAG3: normal values [Letter]. *J Nucl Med* 1995;36:706–708.
17. Tondeur M, Piepsz A, Dobbeleir A, Ham H. Technetium-99m-mercaptoacetyltriglycine gamma camera clearance calculations: methodological problems. *Eur J Nucl Med* 1991;18:83–86.
18. Granerus G, Moonen M. Effects of extra-renal background subtraction and kidney depth correction in the measurement of GFR by gamma camera renography. *Nucl Med Commun* 1991;12:519–527.
19. Shore RM, Koff SA, Mentser M, et al. Glomerular filtration rate in children: determination from the $^{99m}$Tc-DTPA renogram. *Radiology* 1984;151:627–633.
20. Russell CD, Bischoff PG, Kontzen F, et al. Measurement of glomerular filtration rate using $^{99m}$Tc-DTPA and the gamma camera: a comparison of methods. *Eur J Nucl Med* 1985;10:519–521.
21. Peters AM, George P, Ballardie F, Gordon I, Todd-Pokropek AT. Appropriate selection of background for $^{99m}$Tc-DTPA renography. *Nucl Med Commun* 1988;9:973–985.
22. Peters AM, Gordon I, Evans K, Todd-Pokropek A. Background in $^{99m}$Tc-DTPA renography evaluated by the impact of its components on individual kidney glomerular filtration rate. *Nucl Med Commun* 1988;9:545–552.
23. Eshima D, Taylor A. Technetium-99m-mercaptoacetyltriglycine: update on the new $^{99m}$Tc renal tubular function agent. *Semin Nucl Med* 1992;22:61–73.
24. Taylor, A, Nally J, Aurell M, et al. Consensus report on ACE inhibitor renography for the detection of renovascular hypertension. *J Nucl Med* 1996;37:1876–1882.
25. Blaufox MD, Dubovsky EV, Hilson AJW, Taylor A Jr, de Zeeuw R. Report of the working party group on determining the radionuclide of choice. *Am J Hypertens* 1991;4:747S–748S.

# Evaluation of Fulminant Hepatic Failure by Scintigraphy with Technetium-99m-GSA

Susumu Shiomi, Tetsuo Kuroki, Maki Kuriyama, Tadashi Takeda, Shuhei Nishiguchi, Shinya Nakajima, Takashi Tanaka and Hironobu Ochi

*Third Department of Internal Medicine Department of Public Health, and Division of Nuclear Medicine, Osaka City University Medical School, Osaka, Japan*

We evaluated the usefulness of hepatic receptor imaging with $^{99m}$Tc-diethylenetriaminepentaacetic acid galactosyl human serum albumin (GSA) to establish the diagnosis and prognosis of fulminant hepatic failure (FHF). **Methods:** Of the 20 patients, 8 had acute hepatitis and 12 had FHF. Computer acquisition of gamma-camera data started just before the injection of 185 MBq $^{99m}$Tc-GSA and stopped 20 min later. Time-activity curves for the heart and liver were generated from regions of interest (ROIs) for the whole liver and precordium. A receptor index was calculated by division of the radioactivity of the liver ROI by that of the liver plus heart ROIs 15 min after the injection. An index of blood clearance was calculated by division of the radioactivity of the heart ROI at 15 min by that of the heart ROI 5 min after the injection. **Results:** The receptor index was less than 0.83 in all patients with FHF, but it was more than 0.83 in all patients with acute hepatitis. The index of blood clearance was more than 0.72 in all patients with FHF but less than 0.72 in all patients with acute hepatitis. All six survivors of FHF had receptor indices of 0.58 or more, but in five of the six patients who later died, the receptor index was 0.58 or less. The index of blood clearance was 0.85 or less in all survivors but 0.85 or more in the same five patients who later died. **Conclusion:** Hepatic receptor imaging with $^{99m}$Tc-GSA facilitated the evaluation of hepatic function reserve and was useful in establishing the diagnosis and prognosis of FHF.

**Key Words:** technetium-99m-GSA; asialoglycoprotein receptor; fulminant hepatic failure

**J Nucl Med 1997; 38:79–82**

Fulminant hepatic failure (FHF) is a syndrome in which jaundice and hepatic encephalopathy appear within 8 wk of the onset of symptoms in a patient without a history of liver disease (*1*). Survival rates in patients with FHF have improved in recent years, probably because of improvements in intensive care, but mortality remains high (*2*). Various blood biochemical tests have been used for evaluation of hepatic functional reserve (*3,4*), but their results are not always meaningful because patients with FHF may be treated by plasmapheresis and blood product supplementation. Imaging methods such as liver scintigraphy (*5–7*), abdominal CT scanning (*8*) and abdominal ultrasonography (*9*) are useful in the diagnosis of diffuse hepatic diseases such as FHF. Liver scintigraphy with a radiocolloid is the most useful of the three in establishing the diagnosis of FHF. Hepatic receptor imaging with $^{99m}$Tc-diethylenetriaminepentaacetic acid galactosyl human serum albumin (GSA) is a new method for the diagnosis of hepatic disease on the basis of the specific binding of hepatocytes to asialoglycoprotein receptors (*10,11*). We evaluated the clinical usefulness of $^{99m}$Tc-GSA scintigraphy in the diagnosis of FHF and in prediction of the outcome.

## MATERIALS AND METHODS

### Patients

We studied 12 patients with FHF, 8 with acute hepatitis (AH), 50 with chronic hepatitis and 120 with cirrhosis who were admitted to our hospital between April 1993 and October 1995. Patients with chronic hepatitis and cirrhosis were diagnosed by examination of specimens obtained by laparoscopy or needle biopsy done under ultrasonic guidance. The criteria for diagnosis of FHF was hepatic encephalopathy of grade 2 or more within 2 mo of the onset of signs and symptoms of hepatitis, with a plasma prothrombin level of less than 40% or massive or submassive necrosis of the liver found in biopsy or necropsy specimens (*12*). The clinical and laboratory findings of FHF and AH are summarized in Table 1.

The diagnosis was type A FHF if antibodies of the immunoglobulin M class to hepatitis A antigen were detected and type B FHF if both hepatitis B surface antigens and antibodies of the immunoglobulin M class to hepatitis B core antigen were detected. Type C FHF was diagnosed if hepatitis C virus (HCV) RNA was detected. The diagnosis was of FHF with non-A, non-B, non-C hepatitis if none of the following was detected: antibodies of the immunoglob-

Received Dec. 4, 1995; revision accepted May 8, 1996.

For correspondence or reprints contact: Susumu Shiomi, MD, Third Department of Internal Medicine, Osaka City University Medical School, 1-5-7 Asahimachi, Abeno-ku, Osaka 545, Japan.